Research Article | Vol. 28, No. 3 / 3 February 2020 / Optics Express 3352
Optics EXPRESS

Discrimination between two distinct nonlinear effects by polarization-resolved *Z*-scan measurements

MARLON S. MELHADO,[1] TIAGO G. B. DE SOUZA,[1] SERGIO C. ZILIO,[1,2] EMERSON C. BARBANO,[3] AND LINO MISOGUTI[1,*]

[1]*Instituto de Física de São Carlos, Universidade de São Paulo, Caixa Postal 369, 13560-970 São Carlos, SP, Brazil*
[2]*Instituto de Física, Universidade Federal de Goiás,74001-970, Goiânia, GO, Brazil*
[3]*Departamento de Física, Universidade Federal do Paraná, 81531-980, Curitiba, PR, Brazil*
[*]*misoguti@ifsc.usp.br*

Abstract: We investigated how the *Z*-scan technique can be explored to distinguish two types of nonlinear refractive effects by employing two distinct laser polarizations. It is possible that pure electronic, molecular orientation and thermal nonlinear effects may occur simultaneously during light-matter interaction. We found a way to discriminate and quantify two distinct nonlinear processes from *Z*-scan signals measured with linear and circular polarizations. This paper provides analytical equations for nonlinear refractions and in order to test them, we carried out measurements in CS_2 and in a rhodamine-B solution, where electronic and orientational, and electronic and thermal nonlinearities mixing, respectively, are present.

1. Introduction

In the nonlinear optical interaction between light and matter, it is possible that distinct nonlinear effects occur simultaneously, resulting in a single effective nonlinear response. The type and the strength of each nonlinear effect depend on light and matter properties. For instance, they may depend on the laser pulse width, wavelength, repetition rate, energy and, also, on the linear and nonlinear optical absorption of the sample. Therefore, in order to perform correct nonlinear optical measurements, it is crucial to know the eventual existence of nonlinear effects mixture and, more important, how to discriminate them. In fact, there are several studies on this subject using optical Kerr effect, transient grating, etc. [1–7]. For example, considering that different nonlinear effects have distinct response time, time-resolved methods can be applied to distinguish such contributions. These methods are successful because the pure electronic effect is nearly instantaneous, while nuclear contributions such as molecular re-orientation are non-instantaneous [8]. Unfortunately, these methods are usually complex and employ two-beams and sometimes even three beams, in pump-probe configurations. Although they are very good for response time determination, they are not so precise for absolute magnitude determination. On the other hand, it is possible to use a single beam configuration to measure the nonlinear effect mixture, but in this case, it is necessary to perform measurements with several pulse widths. Indeed, we have recently measured solvents presenting an effective nonlinear refractive index, $n_{2,eff}$, due to contributions of two mechanisms: electronic and molecular orientation. They could be discriminated by means of nonlinear ellipse rotation (NER) measurements as a function of pulse width [9]. This method works well because for short (long) pulses, $n_{2,eff}$ is predominantly dominated by the electronic (orientational) nonlinearity, which is an instantaneous (a non-instantaneous) effect. In this case, an empirical equation fitting the dependence of $n_{2,eff}$ as a function of the pulse width provides the strength and time dependence of the two nonlinear processes.

#378270 https://doi.org/10.1364/OE.378270
Journal © 2020 Received 17 Sep 2019; revised 15 Dec 2019; accepted 12 Jan 2020; published 24 Jan 2020

Optics EXPRESS

The present work proposes a simple analytical solution to discriminate two distinct nonlinear effects with a single-beam configuration, just by exploring polarization-resolved Z-scan measurements. Usually, a linearly polarized laser beam is used to measure the refractive Z-scan signal (ΔT_{pv}) [10]. However, it is also interesting to measure ΔT_{pv} using circular polarization [11] because in this case, ΔT_{pv} can change by a certain factor that depends on the origin of the third-order nonlinearity. For the sake of simplicity, we will consider three types of nonlinearities: electronic, orientational and thermal, which for circular polarization have ΔT_{pv} modified by a factor of: 1.5, 4, and 1, respectively, when compared to that obtained with linear polarization [12]. Therefore, in the presence of just one nonlinear effect, ΔT_{pv} changes according to these factors, but in the case of two or more nonlinear effects ΔT_{pv} assumes an intermediate value that depends on the contribution of each nonlinearity. Indeed, considering that each nonlinear effect is independent and contributes additively to the effective ΔT_{pv}, we can write the contribution of each signal from different origin, separately and independently [8]. This independence makes possible to predict the effective ΔT_{pv} signals for linear and circular polarization.

Taking into account these simple rules, we propose a theoretical solution for three cases of mixing: electronic and orientational, electronic and thermal and orientation and thermal effects, which, as a proof of concept, were experimentally tested for the first two cases. Yet, we couldn't find any situation for the orientational and thermal mixing case. For the case of mixing of electronic and orientational effects we measured Z-scan signals of CS_2 solvent as a function of laser polarization and pulse width, because we know that for most of solvents, the contribution of the orientational nonlinearity depends on the pulse width. For the second case (electronic and thermal nonlinearities), we measured a rhodamine B (RB) solution with the laser frequency tuned near the resonance band because it is expected that thermal effects appear in this situation. Here we have considered the thermal effect as the one more likely to be responsible for the nonlinear refraction signal along with the electronic one, but without losing the main message of our work, other "isotropic" non-tensorial effects such as electrostriction, resonant nonlinear absorption, etc. can also occur.

2. Nonlinear refraction

2.1. Nonlinear refraction

There are several mechanisms that give rise to the third-order nonlinear refractive index, n_2. In general, n_2 can be treated as a scalar whose mathematical description relies on the optical Kerr effect, where the refractive index is intensity-dependent according to: $n = n_0 + n_2 I = n_0 + \Delta n$, where n_0 is the linear refractive index and I is the laser irradiance. More accurately, n_2 is connected to the nonlinear polarization, which is related to the third-order nonlinear susceptibility tensor $\chi^{(3)}_{ijkl}$, and consequently, dependent on the crystalline form and orientation, laser polarization, etc. For isotropic materials such as liquids, the number of elements is reduced to two independent coefficients A ($=6\chi_{1122}$) and B ($=6\chi_{1221}$) [12].

Thus, in Z-scan measurements with different laser polarizations, it is necessary to consider such tensor nature of the third-order nonlinear susceptibility. Also, it is important to point out that the ratios between these two coefficients are different for the pure nonresonant electronic ($B/A = 1$), orientational ($B/A = 6$) and thermal ($B/A = 0$) nonlinearities. In this way, considering that for different polarization states, A and B coefficients are excited differently, it is possible to predict how ΔT_{pv} will be affected by the laser polarization and physical origin of the nonlinearity. Z-scan measurement as a function of laser polarization is not new and it was used to determine if different nonlinear effects are present in a particular case [8,11]. However, as far as we know, no one has derived analytical equations relating the signals measured for different polarizations with the origin of the nonlinearities.

Optics EXPRESS

2.2. Nonlinear refraction for linear and circular polarization

The change in the refractive index, Δn, of a Kerr medium is given by [12]:

$$\Delta n_{linear} = \frac{I}{4n_0^2\varepsilon_0 c}\left(A + \frac{1}{2}B\right), \tag{1}$$

for linear polarized light and

$$\Delta n_{circular} = \frac{I}{4n_0^2\varepsilon_0 c}A, \tag{2}$$

for circular polarized light, where $\epsilon_0 = 8.85 \times 10^{-12}$ F/m is the vacuum electrical permittivity, c is the speed of light in vacuum and the laser irradiance I is considered to be the same for linear and circular polarizations. Using Eqs. (1) and (2) and the ratios between the coefficients A and B, we observe that $\Delta n_{linear}/\Delta n_{circular}=1 + B/(2A) = 3/2$, 4 and 1 for pure electronic (*elec*), orientational (*ori*) and thermal (*ther*) nonlinearities, respectively. In the case of a mixture of two nonlinear processes, the ratio will not be these but rather weighted values.

2.3. Z-scan signals for linear and circular polarization

The Z-scan signal measured with linearly polarized light depends on both A and B, and for circular polarization it depends only on A [12]. In the Z-scan trace, the difference between its peak and its valley (ΔT_{pv}) is proportional to Δn, according to: $\Delta T_{pv}=0.406kL\Delta n$ [10], where k is the wave vector and L is the sample thickness for the case of negligible linear absorption. The linear relation between ΔT_{pv} and Δn explains why $(\Delta T_{pv})_{linear}/(\Delta T_{pv})_{circular}= \Delta n_{linear}/\Delta n_{circular}$. For the mixing of electronic and orientational nonlinearities we can express the Z-scan signal as a sum of two independent contributions, as shown in Eq. (3). When circular polarized light is used, there is a reduction in the signal that is expressed in Eq. (4):

$$(\Delta T_{pv})_{linear} = \Delta T_{pv}^{elec} + \Delta T_{pv}^{ori}, \tag{3}$$

$$(\Delta T_{pv})_{circular} = \frac{2}{3}\Delta T_{pv}^{elec} + \frac{1}{4}\Delta T_{pv}^{ori}, \tag{4}$$

Consequently,

$$\Delta T_{pv}^{elec} = -\frac{3}{5}(\Delta T_{pv})_{linear} + \frac{12}{5}(\Delta T_{pv})_{circular}, \tag{5}$$

$$\Delta T_{pv}^{ori} = \frac{8}{5}(\Delta T_{pv})_{linear} - \frac{12}{5}(\Delta T_{pv})_{circular}, \tag{6}$$

Finally, from the ΔT_{pv} obtained with Eqs. (5) and (6), it is possible to determine the values of n_2 for the electronic and the orientational nonlinearities by considering the usual small aperture approximation for the phase change, $\Delta\phi$, occurring during the propagation in a nonlinear medium [10]:

$$\Delta T_{pv} = 0.406\Delta\phi = 0.406kn_2LI. \tag{7}$$

Similarly, for the mixing of other nonlinear effects such as electronic and thermal nonlinearities, we have:

$$(\Delta T_{pv})_{linear} = \Delta T_{pv}^{elec} + \Delta T_{pv}^{ther}, \tag{8}$$

$$(\Delta T_{pv})_{circular} = \frac{2}{3}\Delta T_{pv}^{elec} + \Delta T_{pv}^{ther}, \tag{9}$$

and, consequently,

$$\Delta T_{pv}^{elec} = 3(\Delta T_{pv})_{linear} - 3(\Delta T_{pv})_{circular}, \tag{10}$$

$$\Delta T_{pv}^{ther} = -2(\Delta T_{pv})_{linear} + 3(\Delta T_{pv})_{circular}. \tag{11}$$

Optics EXPRESS

For orientational and thermal nonlinearities, we have:

$$(\Delta T_{pv})_{linear} = \Delta T_{pv}^{ori} + \Delta T_{pv}^{ther}, \tag{12}$$

$$(\Delta T_{pv})_{circular} = \frac{1}{4}\Delta T_{pv}^{ori} + \Delta T_{pv}^{ther}, \tag{13}$$

and, consequently,

$$\Delta T_{pv}^{ori} = \frac{4}{3}(\Delta T_{pv})_{linear} - \frac{4}{3}(\Delta T_{pv})_{circular}, \tag{14}$$

$$\Delta T_{pv}^{ther} = -\frac{1}{3}(\Delta T_{pv})_{linear} + \frac{4}{3}(\Delta T_{pv})_{circular}. \tag{15}$$

As can be seen, ΔT_{pv} signal due to thermal effect is the same for linear and circular polarization. This simple model leads to the set of analytical Eqs. (5) and (6), (10) and (11), (14) and (15), which is interesting to be tested. We chose to measure CS_2 because it is widely used as a nonlinear optical media for calibration and possesses large electronic and orientational nonlinearities [8,9]. Also, depending on the pulse width, the amount of orientational nonlinearity changes [8,9,13], being ideal for testing Eqs. (5) and (6). On the other hand, we chose to characterize the RB solution because it has a strong electronic nonlinear refraction near the linear resonance band [14] and where, some thermal nonlinearity contribution is expected. In this case, Eqs. (10) and (11) can be tested.

3. Polarization-resolved *Z*-scan

3.1. *Z*-scan setup

The polarization-resolved *Z*-scan used for refractive measurements is very similar to the conventional closed aperture *Z*-scan setup [10] except for the introduction of a broadband quarter waveplate ($\lambda/4$) to control the polarization state, as Fig. 1 shows. In the *Z*-scan method, samples are scanned in the focus region along the beam's propagation direction (z-axis) using a computer-controlled translation stage. Negative values of z correspond to locations of the sample between the focusing lens and its focal plane. A single photodetector with an adjustable aperture in front of it was placed in the far-field region. The aperture size having a radius r_a is related to the linear aperture transmittance by $S = [1\text{-}exp(-2{r_a}^2/{w_a}^2)]$, with w_a denoting the beam radius at the aperture for a very low incident power. By scanning the sample though the focus region ($z = 0$), the normalized transmittance can be measured on the photodetector. The use of an aperture corresponds to $S < 1$ (closed-aperture), which is employed to determine n_2, while $S = 1$ (open-aperture) is used for the determination of nonlinear absorption. A commercial Ti:sapphire chirped-pulse-amplified laser system (Dragon, K&M Labs) delivers pulses at 800 nm, with 2 mJ of output energy at 1 kHz repetition rate. The laser system has an internal grating pulse compressor that can change the pulse width from ~60 fs up to ~2 ps [9]. By using a lens with $f = 20$ cm we obtain a beam waist of about 30 µm. Also, as tunable fs laser pulses, we used a commercial optical parametric amplifier system (TOPAS PRIME, ~100 fs pulse width, 400 nm up to 2600 nm) pumped by the Dragon laser. Silica cuvettes with 2 mm pathlength were used to hold the CS_2 solvent and the RB solution with concentration of about 2×10^{-2} Molar in methanol. In these two cases, we have considered that the nonlinearity of silica is much smaller than those of CS_2 and RB solution, and so, the contribution of the cuvette walls to the effective ΔT_{pv} signals can be neglected.

3.2. *Z*-scan results

Firstly, we measured CS_2 in order to discriminate between electronic and orientational processes. We measured *Z*-scan signals with linear and circular polarizations for different pulse widths.

Optics EXPRESS

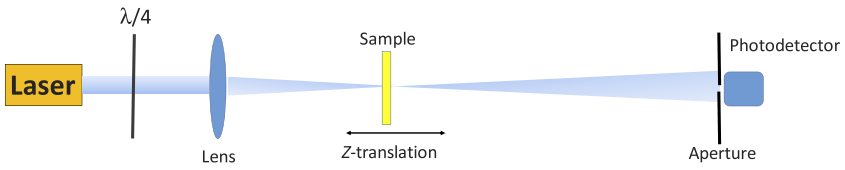

Fig. 1. Schematic diagram of polarization-resolved Z-scan setup which is similar to the original closed-aperture Z-scan with the addition of a quarter-waveplate to control the polarization state of the laser beam (linear and circular polarizations).

Figure 2 shows curves for the shortest and longest pulses, 60 fs and 1.8 ps, respectively. The pulse width as a function of the pulse compression setting in our laser system was previously calibrated with nonlinear ellipse rotation and autocorrelation measurements [9]. Due to the pulse width measurement uncertainty and dispersion in the lens and neutral filter, we estimate that the error in the pulse width is about 10%. For each pulse width we have two ΔT_{pv} signals, one for linear and another for circular polarization, and the results are summarized in Table 1. We started with the shortest pulse width (~60 fs), whose irradiance was about 8.3 GW/cm^2 (P~8 μW), and observed that as the pulse gets longer, the Z-scan signal decreases. We compensated this reduction of the ΔT_{pv} signal by controlling the pulse energy with calibrated neutral filters in order to avoid working with small ΔT_{pv} signals, a condition where the noise can disturb the observation of characteristic Z-scan dispersion curves. There was no observable signal corresponding to nonlinear absorption, which is characterized by the distortion in the refractive Z-scan signal (valley stronger than the peak), indicating a negligible imaginary nonlinear susceptibility. Due to the large number of measurements, we saved time by performing Z-scan measurements only near the $z = 0$ region, where full ΔT_{pv} signals can be acquired and fitted with well-known refractive Z-scan equation [10]. Although some of the fitting curves have not perfectly matched the experimental data, especially in the region away from the focal plane (larger z position), ΔT_{pv} signals could be well determined. Better Z-scan curves can be obtained with more careful alignments and carrying out more measurements, but it would not change the general result.

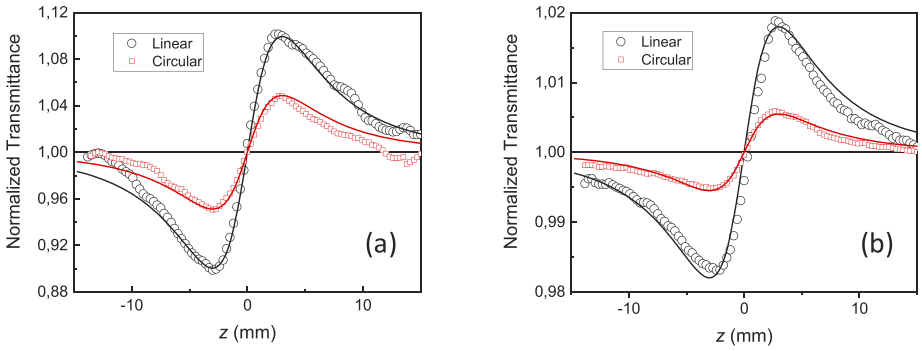

Fig. 2. CS_2 normalized transmittance obtained with refractive Z-scan measurements for linear and circular polarization at pulse widths (a) τ=~60 fs and (b) ~1.8 ps. Although the signal for long pulse was obtained with higher energy, we plotted the normalized signal expected for the same energy used in (a). The solid line is the theoretical fitting based on the refractive Z-scan equation given in Ref. [10].

Figure 3(a) summarizes all ΔT_{pv} signals measured with linear and circular polarizations for different pulse widths. As one can see, both signals decrease because the laser irradiance reduces

Optics EXPRESS

Table 1. Experimental ΔT_{pv} obtained with linear and circular polarizations, whose ratio (lin/circ) changes from ~1.8 up to ~3.0, from short to long pulses, respectively, indicating the mixture of electronic and orientational nonlinearities. Using Eqs. (5) and (6) allows to obtain the respective ΔT_{pv} for electronic (*elec*) and orientational (*ori*) nonlinearities. Finally, Eq. (7) provides the respective nonlinear refraction. The errors from signal fluctuations were estimated to be about 13%. The raw numbers presented here, obtained from appropriate equations, were not rounded to fulfill the estimated 13% error. The unit of n_2 is in $\times 10^{-19}$ m^2/W.

τ(ps)	ΔT_{pv}(lin)	ΔT_{pv}(circ)	Ratio (R) (lin/circ)	ΔT_{pv}(elec)	ΔT_{pv}(ori)	n_2 (elec)	n_2 (ori)
0.060	0.168	0.095	1.77	0.127	0.041	2.39	0.77
0.066	0.153	0.083	1.84	0.107	0.046	2.22	0.94
0.083	0.128	0.071	1.80	0.094	0.034	2.45	0.90
0.111	0.121	0.058	2.09	0.067	0.054	2.32	1.90
0.192	0.109	0.045	2.42	0.043	0.066	2.56	3.99
0.296	0.091	0.036	2.53	0.032	0.059	2.95	5.50
0.416	0.079	0.030	2.63	0.025	0.054	3.21	7.09
0.544	0.069	0.025	2.76	0.019	0.050	3.18	8.60
0.679	0.063	0.022	2.86	0.015	0.048	3.20	10.23
0.819	0.058	0.020	2.90	0.013	0.045	3.39	11.50
0.961	0.054	0.018	3.00	0.011	0.043	3.25	13.02
1.105	0.052	0.018	2.89	0.012	0.040	4.16	13.86
1.251	0.050	0.017	2.94	0.011	0.039	4.24	15.38
1.398	0.047	0.016	2.94	0.011	0.034	5.00	14.73
1.546	0.045	0.016	2.81	0.012	0.033	5.63	16.00
1.694	0.041	0.015	2.73	0.011	0.030	6.06	15.73
1.844	0.036	0.012	3.00	0.007	0.029	4.16	16.65

for longer pulses. With these two signals, and by using Eqs. (5) – (7), we obtained the respective electronic and orientational nonlinear refractions, as depicted in Fig. 3(b).

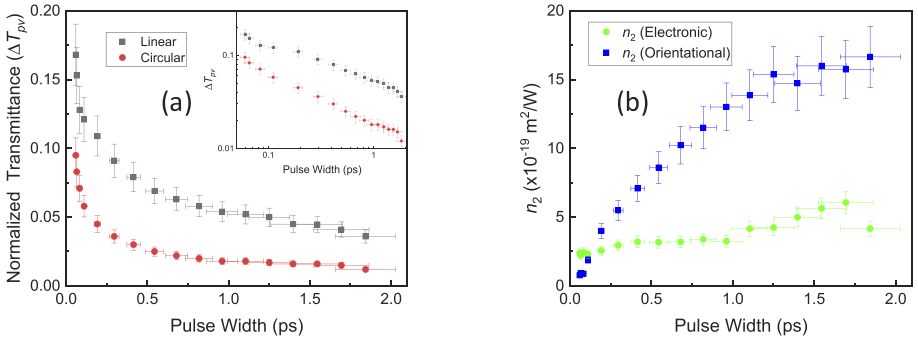

Fig. 3. (a) CS_2 normalized transmittance at 800 nm obtained with refractive Z-scan measurements at different pulse widths. In the inset, the same data in *log-log* scale. (b) Nonlinear refractive indices of CS_2 obtained with our polarization-resolved Z-scan measurements.

It is possible to observe in Fig. 3(b) that the electronic nonlinearity is nearly constant while the orientational nonlinearity grows as the pulse width increases. There is a small growth tendency in the electronic nonlinearity value that is probably due to the pulse width determination error [9]. The CS_2 electronic nonlinearity found in the literature is about 2.5×10^{-19} m^2/W, similar

Optics EXPRESS

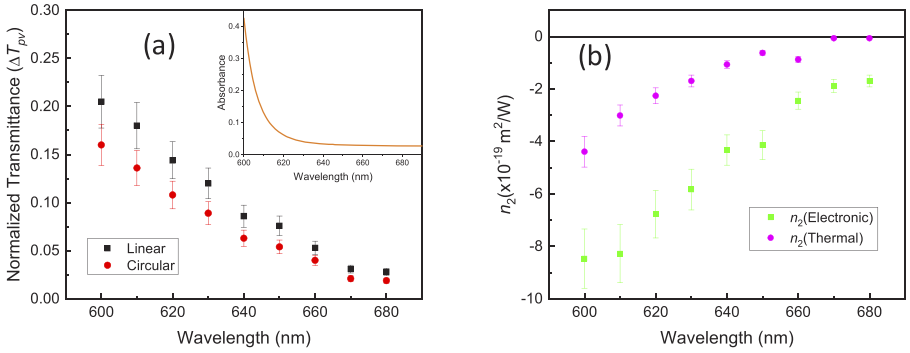

Fig. 4. (a) Normalized transmittance obtained with refractive Z-scan measurements in a RB solution for different wavelengths. In the inset, it is the linear absorption curve of measured solution. (b) Nonlinear refractive indices for the RB solution obtained with our polarization-resolved Z-scan measurements.

to that observed in our data [8,15]. Although we supposed beforehand the presence of both electronic and orientational nonlinearities in CS_2, the ratios between ΔT_{pv} obtained with linear and circular polarizations confirmed our hypothesis. The experimental ratios ranged from about 1.7 to 3.0, from short to long pulse widths, as expected for the transition from electronic ($R = 1.5$) to orientational ($R = 4$) nonlinear effects.

For the second case, we measured Z-scan signals in a RB solution as a function of the wavelength (Fig. 4). We employed tunable wavelength pulses delivered by an OPA pumped by 1 kHz Ti:sapphire Dragon laser system. We carried out measurements from 600 nm to 680 nm where the RB solution is very transparent and no significant nonlinear absorption is present [16]. As seen in Table 2, the ΔT_{pv} ratios ranged between about 1.3 and 1.5, from short to long wavelengths, respectively. According to our model, these smaller values indicate that the dominant electronic nonlinearity ($R = 1.5$) is affected gradually by the thermal nonlinearity ($R = 1$) as the pump wavelength gets close to the absorbance band (λ_{peak}~543 nm). It is also important to notice that both electronic and thermal nonlinearities are negative in this range. It is well known that the thermal effect contributes with a negative signal [10,17] and also,

Table 2. Experimental ΔT_{pv} obtained with linear and circular polarizations, whose ratio (*lin/circ*) changes from ~1.3 (600 nm) to ~1.5 (680 nm), indicating the presence of electronic and thermal nonlinearities. Using Eqs. (10) and (11) we obtain ΔT_{pv} for electronic (*elec*) and thermal (*ther*) nonlinearities. Finally, Eq. (7) provides the respective nonlinear refractions. The errors from signal fluctuations were estimated to be about 13%. The raw numbers presented here, obtained from appropriate equations, were not rounded to fulfill the estimated 13% error. The unit of n_2 is $\times 10^{-19}$ m^2/W.

λ(nm)	ΔT_{pv}(lin)	ΔT_{pv}(circ)	Ratio (R) (lin/circ)	ΔT_{pv}(elec)	ΔT_{pv}(ther)	n_2 (elec)	n_2 (ther)
600	0.205	0.160	1.28	0.135	0.070	-8.467	-4.390
610	0.180	0.136	1.32	0.132	0.048	-8.279	-3.011
620	0.144	0.108	1.33	0.108	0.036	-6.774	-2.258
630	0.120	0.089	1.35	0.093	0.027	-5.833	-1.693
640	0.086	0.063	1.36	0.069	0.017	-4.328	-1.066
650	0.076	0.054	1.41	0.066	0.010	-4.140	-0.627
660	0.053	0.040	1.33	0.039	0.014	-2.446	-0.878
670	0.031	0.021	1.47	0.030	0.001	-1.882	-0.063
680	0.028	0.019	1.47	0.027	0.001	-1.693	-0.063

Optics EXPRESS

the negative nonlinearity obtained here for the electronic n_2 for this wavelength range is in accordance to recent data [14]. Furthermore, the decreasing of the electronic nonlinearity for longer wavelengths is compatible to what is expected for the case of RB at this wavelength range. Finally, the thermal contribution tends to decrease as the laser wavelength gets far from the linear absorption band. As mentioned, other isotropic effects where $B = 0$, besides thermal, may also be responsible for these results.

We also worked with lower irradiances, of about 2.5 GW/cm^2 (P~4 μW) for all wavelengths, in order to avoid any significant refractive Z-scan signals of pure solvent and cuvette. Indeed, the small positive cuvette (n_2~2.8×10^{-20} m^2/W) and solvent (methanol) (n_2~4.6×10^{-20} m^2/W) [9] refractive nonlinearities may have slightly affected the obtained negative electronic and thermal values in Table 2. However, in this simple preliminary study we have not considered this issue yet. In addition, other nonlinear absorption effects such as: two-photon absorption (2PA) [16], saturable (SA) and reverse saturable absorption (RSA), etc. in this wavelength range [18] can be present but were not taken into account.

4. Conclusions

In conclusion, we proposed simple analytical equations, capable of separating the contributions of two distinct nonlinearities among electronic, orientational and thermal, by the use of linear and circular polarized laser beams. This is possible because of the different polarization dependence of the Z-scan signals, which can be explained by the tensor nature of the third-order nonlinear susceptibility, B and A, and their respective ratios (1, 6 and 0), that depend on the mechanism which originates the nonlinear refraction (electronic, orientational and thermal, respectively). As a proof of concept, we have used this method to measure the electronic and molecular orientational nonlinearity in CS_2 as well as the electronic and thermal nonlinearity in a rhodamine B solution. It is important to point out that even though we have observed two positive and two negative nonlinearities for CS_2 and RB, respectively, our model has no restriction for other sign mixing cases. Here, we have considered for simplicity these three common and well-known nonlinear effects, but without losing the proposed idea, other cases of mixing can also be studied.

Funding

Fundação de Amparo à Pesquisa do Estado de São Paulo (2018/11283-7, 2019/00638-1); Conselho Nacional de Desenvolvimento Científico e Tecnológico (465763/2014-6,409258/2018-0).

Acknowledgments

We acknowledge financial support from the Brazilian Conselho Nacional de Desenvolvimento Científico e Tecnológico (CNPq), Coordenação de Aperfeiçoamento de Pessoal de Nível Superior (CAPES) and Fundação de Amparo à Pesquisa do Estado de São Paulo (FAPESP).

Disclosures

The authors declare that there are no conflicts of interest related to this article.

References

1. D. McMorrow, W. T. Lotshaw, and G. A. Kenney-Wallace, "Femtosecond optical Kerr studies on the origin of the nonlinear responses in simple liquids," IEEE J. Quantum Electron. **24**(2), 443–454 (1988).
2. T. Steffen, J. T. Fourkas, and K. Duppen, "Time resolved four- and six-wave mixing in liquids 2. Experiments," J. Chem. Phys. **106**(10), 3854–3864 (1997).
3. P. P. Ho and R. R. Alfano, "Optical Kerr effect in liquids," Phys. Rev. A **20**(5), 2170–2187 (1979).
4. Q. Zhong and J. T. Fourkas, "Optical Kerr effect spectroscopy of simple liquids," J. Phys. Chem. B **112**(49), 15529–15539 (2008).
5. M. Falconieri, "Thermo-optical effects in Z-scan measurements using high-repetition-rate lasers," J. Opt. A: Pure Appl. Opt. **1**(6), 662–667 (1999).

Optics EXPRESS

6. A. Gnoli, L. Razzari, and M. Righini, "*Z*-scan measurements using high repetition rate lasers: how to manage thermal effects," Opt. Express **13**(20), 7976–7981 (2005).
7. L. Misoguti, C. R. Mendonça, and S. C. Zilio, "Characterization of dynamic optical nonlinearities with pulse trains," Appl. Phys. Lett. **74**(11), 1531–1533 (1999).
8. M. Reichert, H. Hu, M. R. Ferdinandus, M. Seidel, P. Zhao, T. R. Ensley, D. Peceli, J. M. Reed, D. A. Fishman, S. Webster, D. J. Hagan, and E. W. Van Stryland, "Temporal, spectral, and polarization dependence of the nonlinear optical response of carbon disulfide," Optica **1**(6), 436–445 (2014).
9. M. L. Miguez, T. G. B. de Souza, E. C. Barbano, S. C. Zilio, and L. Misoguti, "Measurement of third-order nonlinearities in selected solvents as a function of the pulse width," Opt. Express **25**(4), 3553 (2017).
10. M. Sheik-Bahae, A. A. Said, T. Wei, D. J. Hagan, and E. W. Van Stryland, "Sensitive measurement of optical nonlinearities using a single beam," IEEE J. Quantum Electron. **26**(4), 760–769 (1990).
11. X. Q. Yan, Z. B. Liu, X. L. Zhang, W. Y. Zhou, and J. G. Tian, "Polarization dependence of *Z*-scan measurement: theory and experiment," Opt. Express **17**(8), 6397–6406 (2009).
12. R. W. Boyd, *Nonlinear Optics*, 3rd ed. (Academic 2008).
13. P. Zhao, M. Reichert, S. Benis, D. J. Hagan, and E. W. Van Stryland, "Temporal and polarization dependence of the nonlinear optical response of solvents," Optica **5**(5), 583–594 (2018).
14. M. S. Melhado, E. C. Barbano, M. G. Vivas, S. C. Zilio, and L. Misoguti, "Absolute nonlinear refractive index spectra determination of organic molecules in solutions," J. Phys. Chem. A **123**(4), 951–957 (2019).
15. K. Kiyohara, K. Kamada, and K. Ohta, "Orientational and collision-induced contribution to third-order nonlinear optical response of liquid CS_2," J. Chem. Phys. **112**(14), 6338–6348 (2000).
16. N. S. Makarov, M. Drobizhev, and A. Rebane, "Two-photon absorption standards in the 550-1600 nm excitation wavelength range," Opt. Express **16**(6), 4029–4047 (2008).
17. H. A. Badran, "Thermal properties of a new dye compound measured by thermal lens effect and *Z*-scan technique," Appl. Phys. B: Lasers Opt. **119**(2), 319–326 (2015).
18. N. K. M. Naga Srinivas, S. V. Rao, and D. N. Rao, "Saturable and reverse saturable absorption of rhodamine B in methanol and water," J. Opt. Soc. Am. B **20**(12), 2470–2479 (2003).